K–T boundary spherules from Blake Nose (ODP Leg 171B) as a record of the Chicxulub ejecta deposits

F. MARTÍNEZ-RUIZ[1], M. ORTEGA-HUERTAS[2], I. PALOMO-DELGADO[2] & J. SMIT[3]

[1]*Instituto Andaluz de Ciencias de la Tierra, CSIC-Universidad de Granada, Facultad de Ciencias, Avda. Fuentenueva, s/n. 18002 Granada, Spain (e-mail: fmruiz@goliat.ugr.es)*

[2]*Departamento de Mineralogía y Petrología, Facultad de Ciencias, Universidad de Granada, Avda. Fuentenueva, s/n. 18002 Granada, Spain*

[3]*Department of Sedimentary Geology, Vrije Universiteit, 1081 HV Amsterdam, Netherlands*

Abstract: The Cretaceous–Tertiary (K–T) boundary interval recovered by the ODP Leg 171 at Site 1049 (Blake Nose, NW Atlantic) contains a thick (9–17 cm) spherule bed marking the boundary. The spherules are mainly perfect spheres with a lesser proportion of oval spherules. They usually range from 100 to 1000 μm. This bed represent the diagenetically altered impact ejecta from Chicxulub and further supports this structure as the site of the K–T impact. Mineralogical and geochemical investigations indicate that impact-generated glass was altered to smectite. Transmission electron microscopy observations revealed in some spherules that smectite is forming from a Si-rich or Ca-rich material, which could suggest a precursor similar to Haitian glasses. The variable thickness and the presence of some Cretaceous planktonic foraminifera and clasts of Cretaceous chalk suggest reworking of the ejecta material. However, the spherule bed confirms that a large volume of the Chicxulub ejecta material reached the Blake Nose Plateau.

Introduction

The Ocean Drilling Program (ODP) Leg 171B recovered an excellent Cretaceous–Tertiary (K–T) boundary interval at three locations along Blake Nose (NW Atlantic): Sites 1049, 1050 and 1052. At Site 1049 a spectacular boundary layer was recovered within this interval, providing further evidence supporting the Chicxulub structure as the site for the K–T impact. OPD Site 1049 is located on the eastern margin of Blake Nose and represents the deepest site of the Blake Nose transect, at a present depth of 2671 m below sea level. The boundary layer, mostly consisting of green spherules interpreted to be of impact origin (Norris *et al.* 1998), shows a variable thickness in the three holes drilled at Site 1049. These circumstances suggest reworking of the ejecta material down-slope after deposition. The green spherules are none the less a record of impact-generated material.

The Chicxulub impact originated distinct dispersal phases (e.g. Alvarez *et al.* 1995; Pierazzo & Melosh 1999) mostly derived from: (1) the turbulent front of melted target rocks deposited in the proximity of the crater site, and (2) the vertically expanding hot vapour plume of vaporized bolide with entrained melted target rocks that was dispersed and deposited globally (the fireball layer). Thus, locations proximal to Chicxulub show greater contributions of the ejecta blanket derived from the crater rocks. Drilled holes at Site 1049 would have been located *c.* 2000 km NE of Chicxulub and the boundary spherules would represent proximal ejecta material. The purpose of this paper is therefore to present mineralogical and geochemical data from the K–T boundary spherules from Blake Nose to constrain the source material and postdepositional processes that altered the original composition and the original record of the impact event.

Samples and methods

Mineralogical and geochemical analyses of the K–T boundary spherules were carried on samples from Holes 1049A and 1049B drilled by ODP Leg 171B along the Blake Nose transect in the NW Atlantic (Fig. 1). In the studied interval, the boundary layer occurs at the biostratigraphic boundary between the Cretaceous and the Palaeocene sediments. It sharply

From: KROON, D., NORRIS, R. D. & KLAUS, A. (eds). 2001 *Western North Atlantic Palaeogene and Cretaceous Palaeoceanography*. Geological Society, London, Special Publications, **183**, 149–161.
0305-8719/01/$15.00

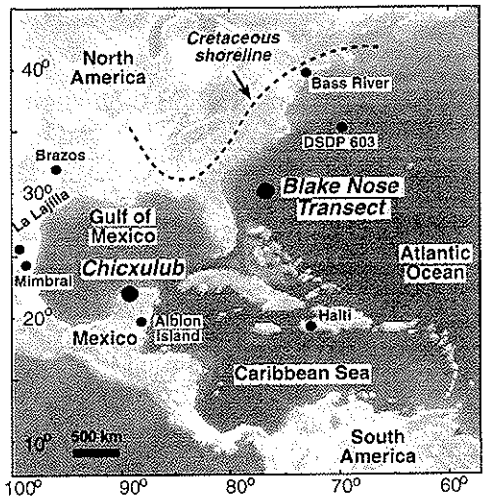

Fig. 1. Location of the Blake Nose transect and some other K–T boundary sections where spherules have been reported.

overlies slumped uppermost Cretaceous foraminiferal–nannofossil ooze (*Abathomphalus mayaroensis* Zone and *Micula prinsii* Zone) and is overlain by Tertiary clay-rich ooze with planktonic foraminiferal assemblages indicative of Early Danian Foraminiferal Zone P-alpha (Norris *et al.* 1998, 1999). This layer, 9–17 cm thick, consists of green spherical and oval-shaped spherules composed of clay as well as some Cretaceous planktonic foraminifera and clasts of Cretaceous chalk (Fig. 2). This spherule bed is capped by a 3 mm thick orange limonite layer that was initially assumed to be the fireball layer (Norris *et al.* 1998). However, the geochemical composition of this limonite layer indicates that it is similar to the rest of the spherule bed except for an enrichment in iron (Martínez-Ruiz *et al.* 2000). This suggests that it is related to only a diagenetic remobilization of iron and that extraterrestrial contribution is not significantly higher.

The spherule bed and sediments above and below were sampled in sections 1049A-17X-2 and 1049B-8H-2, with continuous sampling every 2 cm of the complete interval. Spherules were hand-picked under a stereomicroscope with a dry brush, as spherules in contact with water disintegrate completely. Bulk samples and representative hand-picked spherules were subjected to mineralogical and geochemical analyses using the following methods.

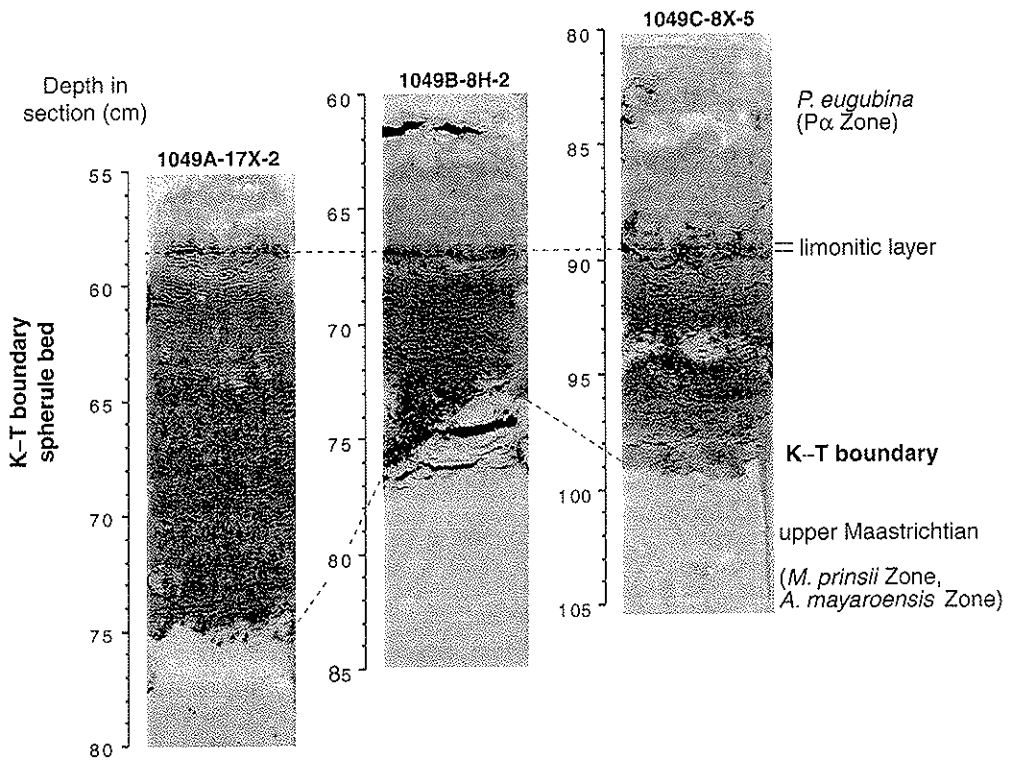

Fig. 2. Core photographs from the K–T boundary layer at Site 1049 for the three holes drilled at this site, showing the variable thickness of the spherule bed and the presence of Cretaceous material within this bed (modified after Norris *et al.* (1998, p. 56)).

X-ray diffraction (XRD)

For bulk mineralogy analyses, samples were packed in Al holders for XRD. For clay mineral analyses, the carbonate fraction was removed using acetic acid, starting the reaction at very low concentration (0.1 mol.$^{-1}$) and increasing to 1 mol.$^{-1}$. Clays were deflocculated by successive washing and the <2 μm fraction was separated by centrifugation. The clay fraction was smeared onto glass slides for XRD. Diffractograms were obtained using a Philips PW 1710 diffractometer with Cu-K_α radiation. Scans were run from 2 to 64° 2θ for bulk samples and untreated clay preparations, and from 2 to 30° 2θ for glycolated, heated and dimethyl-sulphoxide treated samples. Semiquantitative analyses were performed considering the integrated peak area using a specific computer program for the diffractometer used (Nieto *et al.* 1989). The estimated semiquantitative analysis error for bulk-mineralogy absolute values is 5%. For clay-mineral proportions in absolute values, the error ranges from 5 to 10%, but the main aim of the semiquantitative analyses here is to reveal trends in mineral abundance.

Electron microscopy

Morphological studies on bulk samples and hand-picking of spherules were performed using binocular microscopy and scanning electron microscopy (SEM; Zeiss DSM 950). Internal textures were investigated after breaking selected spherules. Quantitative micro-analyses of clay minerals were obtained by transmission electron microscopy (TEM, Philips CM-20 equipped with an EDAX microanalysis system). Quantitative analyses were obtained in scanning TEM mode only from edge particles using a 7 nm diameter beam and 20 × 100 nm scanning area and a short counting time to avoid alkali loss (Nieto *et al.* 1996). Smectite formules were normalized to 11 oxygens.

Blake Nose spherule bed

The spherule bed at Blake Nose (Fig. 2) consists of a coarse, poorly graded and poorly cemented unit. Mineralogical analyses reveal that it is mostly composed of clays and minor proportions of carbonates (Table 1). Other minerals also present in lower proportions are quartz, zeolites and minor amounts of rutile, biotite and some lithic fragments. Clays are mostly smectites, with occasional traces of illite and kaolinite in some of the samples taken from this bed. The contact of the spherule bed with sediments above and below is very sharp. The contact surface of the Cretaceous sediments with the spherule bed contains some spherical impressions (Fig. 3j and k) that seem to be bubbles or deformations by deposition of glassy spherules in soft sediments. The nature of this contact suggests that deposition occurred very rapidly. Cretaceous sediments are slump-folded; however, the overlying stratigraphy is undisturbed. The presence of Cretaceous materials within the spherule bed also suggests downslope transport of the spherule bed material. Deformation of Cretaceous sediments is a general feature at proximal ejecta sites. Deformation and large-scale slope failures were related to the seismic energy input from Chicxulub impact, some of it induced before the emplacement of the ejecta from the same impact (Smit 1999).

Table 1. *XRD semiquantitative data on the main mineral components from the K–T boundary interval at Hole 1049A (see Fig. 2 for location of samples)*

Samples	Depth (mbsf)	Clays	Quartz	Calcite	Dolomite
17X 02 046–048	125.77	9	<5	87	<5
17X 02 048–050	125.79	11	<5	85	<5
17X 02 050–052	125.81	12	<5	84	<5
17X 02 052–054	125.83	11	<5	85	<5
17X 02 054–056	125.85	14	<5	83	<5
17X 02 056–058	125.87	12	<5	85	<5
17X 02 060–062	125.91	75	<5	12	10
17X 02 062–064	125.93	92	<5	6	<5
17X 02 064–066	125.95	90	<5	8	<5
17X 02 066–068	125.97	91	<5	7	<5
17X 02 068–070	125.99	90	<5	8	<5
17X 02 072–074	126.03	91	<5	7	<5
17X 02 074–076	126.05	91	<5	7	<5
17X 02 076–078	126.07	13	<5	84	<5
17X 02 078–080	126.09	23	<5	75	<5
17X 02 080–082	126.11	22	<5	75	<5
17X 02 082–084	126.13	22	<5	74	<5
17X 02 086–088	126.17	21	<5	76	<5
17X 02 088–090	126.17	21	<5	76	<5

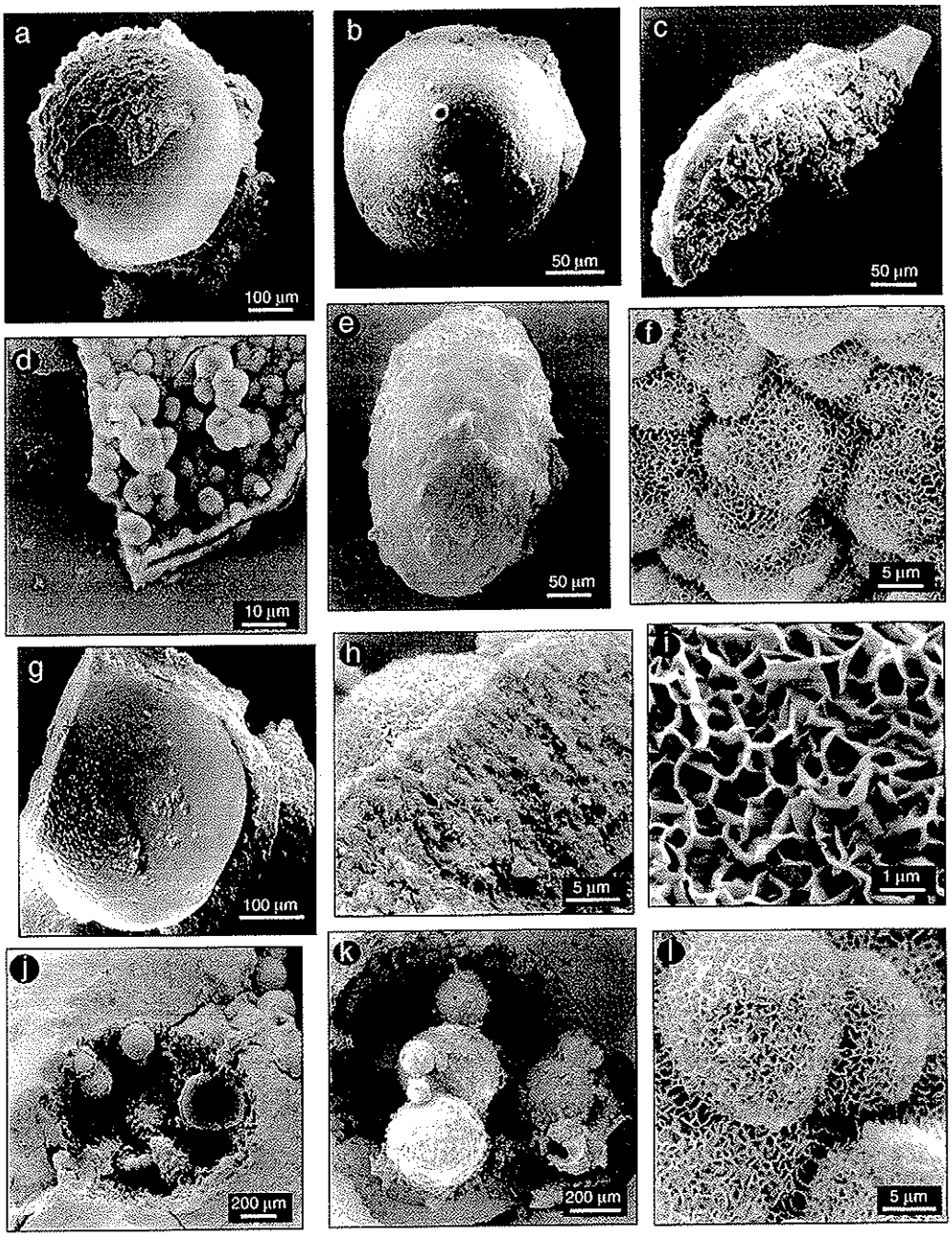

Fig. 3. Scanning electron micrographs of smectite dark green spherules from Blake Nose at Site 1049. (**a**, **b**) View of spherical spherules showing a nodular surface shell ranging from a lumpy surface shell (**a**) to scarce globules on surface (**b**). (**c**) View of a drop-shaped spherule fill with smectite aggregates. (**d**) Enlarged detail of the surface of the spherule shown in (**a**). (**e**) View of an oval spherule with nodular surface. (**f**) Higher-resolution micrographs of the globules from surface spherules showing smectite morphologies. (**g**) Fragment of a hollow spherule showing the inner nodular side and outer lumpy surface. (**h**) Detail of the spherule wall shown in (**g**). (**i**) Higher-resolution micrograph of the smectite wall. (**j**, **k**) Spherical impressions on top of the Cretaceous material filled with spherules with lumpy surfaces. (**l**) Enlarged detail of the lumpy surface of spherules shown in (**j**) and (**k**).

Table 2. *Color, morphology and surface texture of Blake Nose spherules*

	Spherical	Oval	Smooth surface	Rough surface	Nodular surface	Hollow
Light green	X	X		X		
Dark green	X	X		X	X	X
Pale yellow	X		X			X

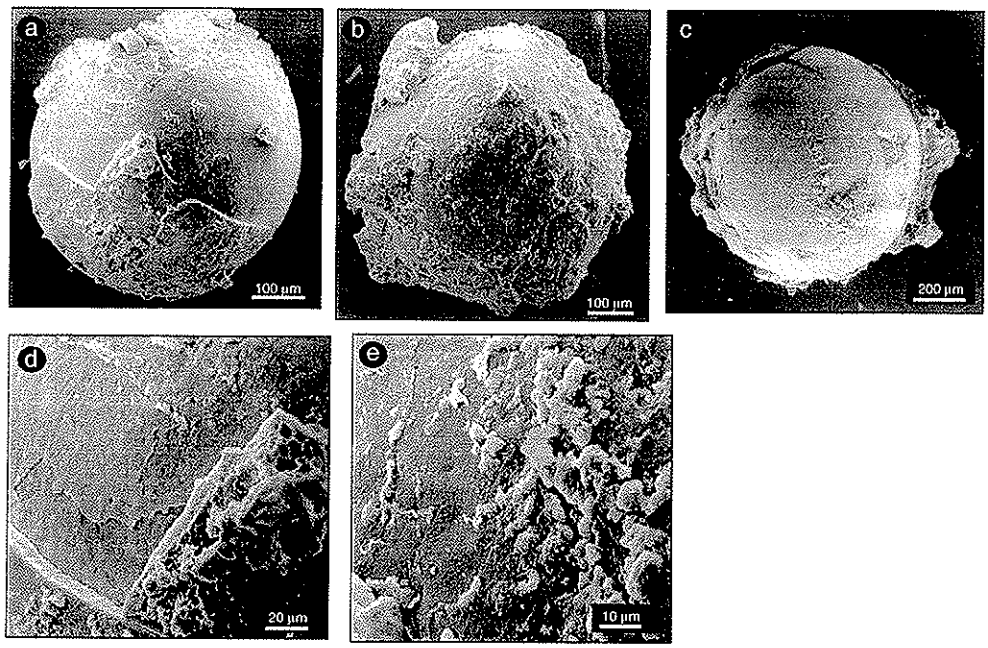

Fig. 4. Scanning electron micrographs of smectite pale yellow spherules from Blake Nose at Site 1049 showing their spherical morphologies (**a–c**) and enlarged details of the surface (**d, e**).

Spherules and diagenetic alteration

Stereomicroscope and SEM observations reveal that the morphologies of the Blake Nose spherules are tektite like and they mainly correspond to perfect spheres and lesser proportions of oval spherules. Size usually ranges from 100 to 1000 µm. Some hollow spherules and spherical voids are filled with smaller spherules (Figs. 3 j and k) that may represent diagenetic infills of original bubbles. Figures 3–5 show some examples of the spherules from the K–T boundary layer at Blake Nose. The surface of the spherules is nodular (Fig 3a, b and e), smooth (Fig 4a–c) or rough (Fig. 5). Different types of spherules have been distinguished based on colour, morphology and surface texture, which are summarized in Table 2.

The smallest dark green spherules (Fig. 3), and occasionally pale yellow ones (Fig. 4), also occur as aggregates (Fig. 3k).The surface of dark green spherules is usually nodular (Fig. 3b), from a few nodules on the surface (Fig. 3b) to a lumpy surface with a nodular aspect (Fig 3d and k). When hollow they are partially or completely filled with aggregates (Fig. 3c). The pale yellow spherules have a smoother outer surface and either are filled with a fine matrix or are hollow with aggregates covering the internal walls, as also occurs in the dark green spherules (Fig. 3g). The light green spherules are massive and present rough surfaces; they are the most abundant (Fig. 5).

Although the morphologies or surfaces of the spherules are different, the XRD scans on oriented samples reveal that spherules are mainly composed of smectite, and no clear evidence for glass relicts has been observed. TEM microanalyses reveal that the smectite corresponds to a dioctahedral type. Compositions are presented in Tables 3 and 4, and Fig. 6. Some compositional variations are observed between dark green spherules and pale yellow spherules (Table 3). Dark green spherules are richer in Fe and pale

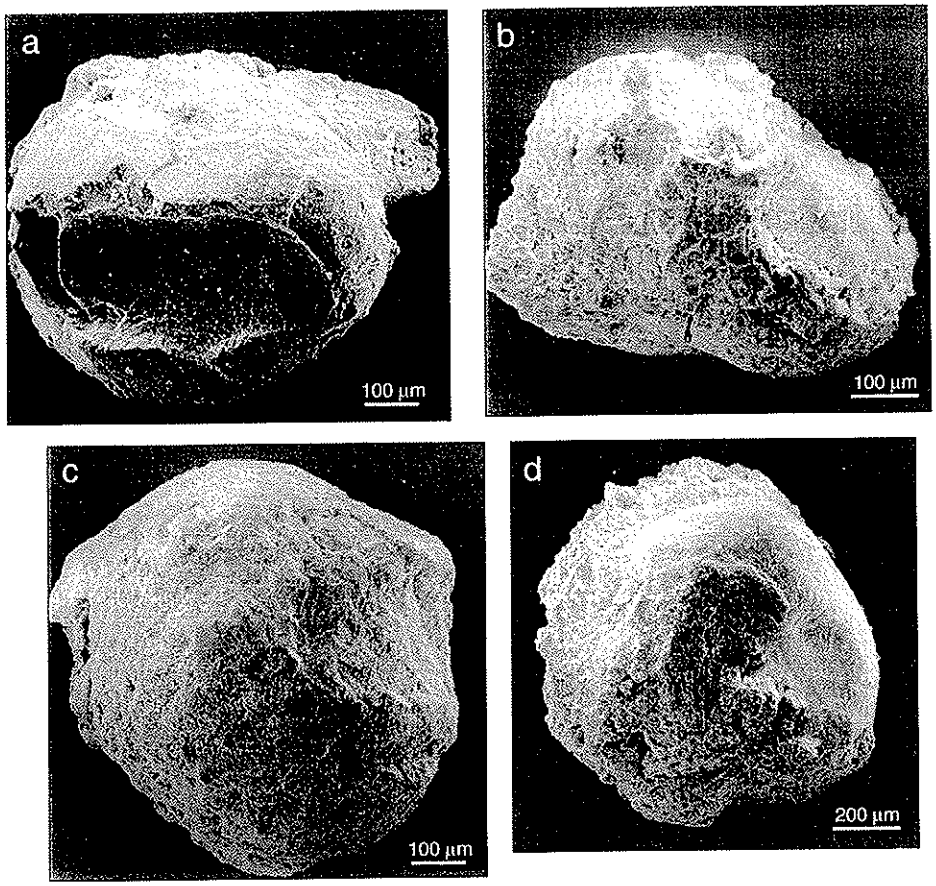

Fig. 5. Scanning electron micrographs of smectite light green spherules from Blake Nose at Site 1049 showing their morphology, size and rough surface.

yellow ones are richer in Ca. These differences may derive from different precursor glass types. In fact, two types of glass occur in the proximal K–T ejecta, black andesitic glass and honey-coloured CaO-rich glass (Izzet 1991; Sigurdsson *et al.* 1991; Smit *et al.* 1992). Precursors of the Blake Nose spherules could then have been similar to those impact glasses. TEM analyses on pale yellow spherules also reveal they contain a very rich-Ca matrix altering to smectite. Some calcite crystals are also observed in this matrix. This calcite could be an original and unaltered phase, but it may also be derived from diagenetic reactions leading to clay authigenesis, such as, for instance, reactions including the formation of palygorskite from smectite and dolomite (Jones & Galán 1988):

$$Ca_{0.25}(Mg_{0.5}Al_{1.5})Si_4O_{10}(OH)_2 + 1.25CaMg(CO_3)_2 + 2SiO_2 = 2Mg_{0.87}Al_{0.75}Si_3O_{7.5}(OH) + 1.5CaCO_3 + CO_2$$

Palygorskite is observed by TEM, suggesting that such reactions could have taken place. Moreover, dolomite and calcite could have been abundant in the ejecta material. The high Ca content could probably derive from carbonate target rocks. In fact, carbonate material is abundant in other K–T ejecta deposits, such as those from Albion Island, Belize, where the ejecta come from the outer portion of the ejecta blanket of the Chicxulub crater. In this formation, abundant clay spheroids are altered impact glass and dolomite spheroids are accretionary lapilli (Pope *et al.* 1999). The differences in composition between spherules suggest therefore that they derive from alteration of a variety of impact glasses and tektite-like material, similar to those reported in the Gulf of Mexico region (Sigurdsson *et al.* 1991; Smit *et al.* 1992; Koeberl & Sigurdsson 1992).

Smectite compositions are also variable within the same spherule; smectites vary from having

Table 3. *Representative AEM data from smectites of the K–T boundary bed at Hole 1049A normalized to* $O_{10}(OH)_2$

Sample	Si	Al^{IV}	Al^{VI}	Mg	Fe	Ti	Σ^{VI}	K	Ca	Na	$\Sigma^{Int.}$
17X-2 58–60	3.78	0.22	1.24	0.49	0.29	0.03	2.05	0.13	0.13	–	0.26
	3.77	0.23	1.73	0.25	0.12	0.00	2.10	0.19	0.01	–	0.20
	3.82	0.18	1.18	0.62	0.40	0.02	2.22	0.08	0.01	–	0.09
	3.96	0.04	1.15	0.43	0.48	0.01	2.07	0.13	0.02	–	0.15
	3.89	0.11	1.31	0.52	0.33	0.00	2.16	0.03	0.04	–	0.07
	3.88	0.12	1.19	0.49	0.43	0.03	2.14	0.08	0.04	–	0.12
	3.90	0.10	1.01	0.45	0.67	0.00	2.13	0.05	0.04	–	0.09
	3.84	0.16	1.22	0.51	0.45	0.00	2.18	0.10	0.02	–	0.12
	3.85	0.15	1.29	0.44	0.42	0.00	2.15	0.13	0.05	–	0.18
17X-2 62–64	3.81	0.19	1.55	0.46	0.16	0.00	2.17	0.07	0.03	–	0.10
	3.78	0.22	1.54	0.52	0.16	0.00	2.22	0.07	0.02	–	0.09
	3.85	0.15	1.64	0.43	0.05	0.00	2.12	0.07	0.03	–	0.10
	3.84	0.16	1.46	0.44	0.23	0.03	2.16	0.06	0.01	–	0.07
	3.87	0.13	1.50	0.43	0.14	0.05	2.12	0.07	0.01	–	0.08
17X-2 68–70	3.63	0.37	1.31	0.84	0.17	0.00	2.32	0.08	0.06	–	0.14
	3.99	0.01	1.63	0.40	0.09	0.00	2.12	0.08	0.00	–	0.08
	3.94	0.06	1.64	0.38	0.11	0.00	2.13	0.02	0.01	–	0.03
	3.95	0.05	1.52	0.35	0.16	0.06	2.09	0.07	0.01	–	0.08
	3.75	0.25	1.44	0.53	0.20	0.03	2.20	0.09	0.06	–	0.15
17X-2 70–72	3.80	0.20	1.47	0.42	0.23	0.03	2.15	0.04	0.02	0.05	0.11
	3.80	0.20	1.55	0.43	0.10	0.04	2.12	0.05	0.05	0.10	0.20
	3.71	0.29	1.53	0.55	0.09	0.06	2.23	0.06	0.02	0.21	0.29
	3.89	0.11	1.44	0.44	0.15	0.05	2.08	0.05	0.03	0.12	0.20
	3.65	0.35	1.36	0.61	0.16	0.12	2.25	0.12	0.02	0.37	0.51
	3.76	0.24	1.28	0.51	0.35	0.00	2.14	0.16	0.01	0.15	0.32
	3.70	0.30	1.50	0.47	0.19	0.00	2.16	0.07	0.04	0.15	0.26
	3.71	0.29	1.21	0.57	0.33	0.00	2.11	0.09	0.04	0.25	0.38
	3.75	0.25	1.38	0.47	0.27	0.02	2.14	0.06	0.19	0.19	0.44
	3.53	0.47	1.28	0.58	0.17	0.09	2.12	0.11	0.15	0.19	0.45
17X-2 74–76	3.58	0.42	1.41	0.33	0.39	0.00	2.13	0.23	0.10	–	0.33
	3.60	0.40	1.42	0.46	0.36	0.00	2.24	0.07	0.03	–	0.10
	3.90	0.10	1.52	0.32	0.27	0.00	2.11	0.05	0.01	–	0.06
	3.80	0.20	1.60	0.31	0.17	0.03	2.11	0.05	0.02	–	0.07
	3.72	0.28	1.65	0.29	0.19	0.00	2.13	0.13	0.03	–	0.16
Dark green spherules	3.57	0.43	1.71	0.49	0.81	0.04	2.05	0.49	0.02	0.18	0.69
	3.67	0.35	1.77	0.41	0.81	0.04	2.03	0.41	0.00	0.12	0.53
	3.66	0.34	1.84	0.48	0.71	0.03	2.06	0.22	0.02	0.25	0.49
	3.56	0.42	1.83	0.53	0.68	0.04	2.08	0.29	0.03	0.27	0.59
	3.77	0.23	1.91	0.44	0.64	0.03	2.02	0.29	0.02	0.08	0.39
Pale yellow spherules	3.64	0.36	1.35	0.50	0.37	0.00	2.22	0.13	0.00	0.07	0.20
	3.64	0.36	1.18	0.39	0.48	0.02	2.07	0.20	0.02	0.16	0.38
	3.69	0.31	1.20	0.39	0.48	0.03	2.10	0.21	0.00	0.16	0.37
	3.56	0.44	1.04	0.48	0.48	0.00	2.00	0.06	0.11	0.48	0.65
	3.76	0.24	1.24	0.40	0.40	0.01	2.05	0.05	0.05	0.13	0.23

–, not determined.
Analyses on single dark green and pale yellow spherules are also presented (see Fig. 2 for location of samples).

normal percentages of Si to being very Si enriched. TEM observations also reveals very high silica areas that do not correspond to a real smectite composition, suggesting that Si-rich glass could have been the precursor. Octahedral cations also present wide ranges of abundance (Tables 3 and 4). The original material is expected to be compositionally variable, as impact-generated glass is only briefly molten and there is not enough time for mixing and homogenizing of the composition (e.g. Alvarez *et al.* 1992).

TEM observations reveal smectite morphologies similar to those of smectites originated from the alteration of volcanic glass (Fig. 7), such as hair-like smectites (Fig. 7a and b) and broad

Table 4. *Representative AEM data from smectites of the K–T boundary bed at Hole 1049B normalized to $O_{10}(OH)_2$ (see Fig. 2 for location of samples)*

Sample	Si	Al^{IV}	Al^{VI}	Mg	Fe	Ti	Σ^{VI}	K	Ca	$\Sigma^{Int.}$
8H-2 68–70	3.76	0.24	1.52	0.53	0.09	0.00	2.14	0.11	0.09	0.20
	3.88	0.12	1.54	0.50	0.14	0.00	2.18	0.02	0.03	0.05
	3.73	0.27	1.37	0.36	0.23	0.00	1.96	0.08	0.32	0.40
	3.86	0.14	1.47	0.35	0.26	0.02	2.10	0.05	0.04	0.09
	3.80	0.20	1.64	0.32	0.13	0.03	2.12	0.03	0.03	0.06
	3.77	0.23	1.44	0.42	0.28	0.02	2.18	0.01	0.03	0.04
	3.91	0.09	1.14	0.18	0.62	0.04	1.98	0.07	0.10	0.17
	3.88	0.12	1.43	0.38	0.28	0.02	2.11	0.04	0.05	0.09
	3.96	0.04	1.63	0.34	0.08	0.03	2.08	0.02	0.02	0.04
	3.95	0.05	1.46	0.37	0.22	0.03	2.08	0.05	0.01	0.06
	3.89	0.11	1.55	0.39	0.17	0.01	2.12	0.04	0.03	0.07
	3.68	0.32	1.09	0.26	0.65	0.07	2.07	0.12	0.08	0.20
	3.79	0.21	1.11	0.13	0.53	0.09	1.86	0.21	0.23	0.44
	3.39	0.61	0.57	0.17	0.09	0.34	1.17	0.25	0.17	0.42
	3.22	0.78	0.46	0.24	1.19	0.10	1.99	0.37	0.23	0.60
	3.35	0.65	0.44	0.16	1.28	0.08	1.96	0.39	0.21	0.60
	3.82	0.18	1.46	0.39	0.25	0.03	2.13	0.06	0.05	0.11
8H-2 70–72	3.84	0.16	1.87	0.14	0.06	0.00	2.07	0.01	0.03	0.04
	3.77	0.23	1.72	0.32	0.03	0.00	2.07	0.02	0.11	0.13
	3.73	0.27	1.43	0.52	0.22	0.05	2.22	0.03	0.02	0.05
	3.94	0.06	1.65	0.29	0.16	0.00	2.10			
	3.75	0.25	1.50	0.45	0.25	0.00	2.20	0.43	0.02	0.45
	3.88	0.12	1.51	0.38	0.21	0.01	2.11	0.07	0.02	0.09
	3.84	0.16	1.53	0.45	0.14	0.02	2.14	0.09	0.02	0.11
	3.83	0.17	1.63	0.34	0.07	0.07	2.11	0.05	0.02	0.07
	3.88	0.12	1.59	0.39	0.12	0.02	2.12	0.05	0.02	0.07
	3.84	0.16	1.40	0.37	0.26	0.02	2.05	0.13	0.09	0.22
8H-2 72–74	3.84	0.16	1.51	0.44	0.20	0.00	2.15	0.07	0.05	0.12
	3.88	0.12	1.45	0.47	0.12	0.06	2.10	0.10	0.05	0.15
	3.79	0.35	1.30	0.41	0.25	0.04	2.00	0.10	0.04	0.14
	3.88	0.12	1.59	0.49	0.07	0.00	2.15	0.05	0.04	0.09
	3.89	0.11	1.64	0.44	0.02	0.00	2.10	0.05	0.09	0.14
	3.75	0.25	1.32	0.53	0.36	0.00	2.21	0.10	0.02	0.12
	3.89	0.11	1.55	0.46	0.16	0.00	2.17	0.04	0.01	0.05

board-shaped smectites (Fig. 7c) (e.g. Chamley 1989). TEM morphological observations have also shown the smectite growing from Si-rich material, probably the altering glass (Fig. 7d) and palygorskite forming from a smectite precursor (Fig. 7e and f). This suggests that smectite directly replaced the original glass phase. At Hole 603B, also located in the NW Atlantic, Klaver *et al.* (1987) proposed that smectite directly replaced the original phase; however, they did not exclude the hypothesis that the smectite represents a second stage of alteration of K–T spherules, after initial alteration to illite. Those workers also considered that the high K_2O content of the smectite might derive from illite. Nevertheless, the TEM observations are in favour of the hypothesis of direct replacement of the original glass. On the other hand, the existence of authigenic palygorskite indicates a high-silica source and alkaline conditions. Couture (1977) reported the association of palygorskite with high-silica minerals such as opal and clinoptilolite and environments with mobilization of silica. In general, high-silica environments favour the precipitation of chain-structure silicates (Beck & Weaver 1978) and smectite can be a precursor of fibrous clays (Singer 1979). Low-temperature alteration of basalts also involves the expulsion of the necessary elements for both fibrous clays and zeolites (Velde 1985). In this case, when the original glass material was altered to smectite, not all the available silica from the former glass was incorporated within the smectite, which favoured the high-silica environments required for the formation of such high-silica minerals. The existence of Ca-rich and Si-rich precursors in some spherules agrees with the geochemistry of Haitian glasses (Izett 1991; Koeberl & Sigurdsson 1992), linked to the Chicxulub crater

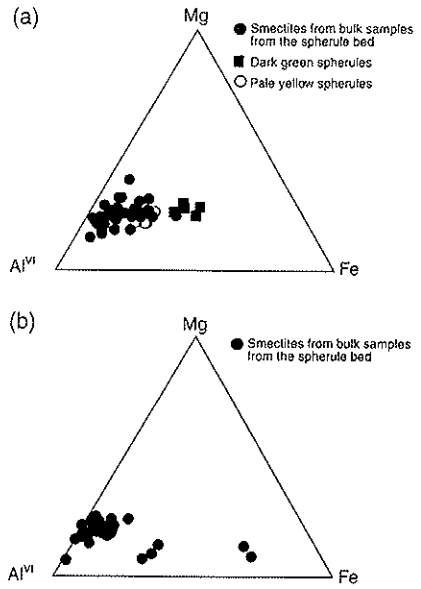

Fig. 6. Al–Fe–Mg diagrams (based on Güven (1988)) showing the smectite composition from spherule bed samples from Holes 1049A (**a**) and 1049B (**b**).

(Swisher *et al.* 1992; Blum *et al.* 1993; Hough *et al.* 1998); however, the pre-impact target stratigraphy would require the presence of Si-rich rocks near the surface (Koeberl 1993) to account for an Si-rich precursor.

Other components

In addition to smectite, the spherule bed also contains minor amounts of calcite, zeolites (Fig. 8), quartz and scarce rutile grains, biotite and some lithic fragments. Calcite mostly derives from the presence of carbonate material in the spherule bed, represented by Cretaceous clast and Cretaceous foraminifera, although some of it could also be represented by the original unaltered ejecta material or authigenic phases. In fact, Ca-rich material has also been observed by TEM in the spherules as discussed above, and stereomicroscope observations also reveal that spherules are macroscopically included in a matrix containing some white patches. SEM analysis confirms that this white matrix is composed of smectite, but also contains calcite and dolomite. Quartz is detrital in origin and shocked quartz is rare in this layer. Rutile and other minor mineral components probably derived from target rock material in a mixture of microfossils, lithic fragments and impact-generated material, labelled by Bralower *et al.* (1998) 'the K–T boundary cocktail'. Zeolites resulted from authigenesis during alteration of the spherule material. Zeolitization requires specific conditions, with temperature, pressure and pH being the most important factors (Hall 1998). The diagenetic conditions of the spherule bed and the geological context preclude high temperature or pressure; pH is thus the most important factor controlling the formation of zeolites during the alteration of the ejecta material. Although not very abundant (< 5 %), zeolites are not common in other K–T boundary layers and therefore provide in this case some constraints on the diagenetic evolution of the boundary material. The Chicxulub impact resulted in acid conditions, as reported by many workers (Hildebrand *et al.* 1991; Sigurdsson *et al.* 1992; Sharpton *et al.* 1993). Increased weathering induced by acid rain has been proposed to explain the crustal Sr enrichment in the oceans at the K–T boundary (MacDougall 1988; Martin & MacDougall 1991). However, large volumes of acid were consumed by reactions with the impact ejecta (e.g. Retallack 1996) and in the boundary deposits, reactions within the ejecta buffered the pH to alkaline conditions. The large contribution of carbonate material from the impact site also favoured such conditions and during alteration of the ejecta material raised pH, allowed zeolitization to take place.

Interpretations and comparison with other K–T ejecta deposits

The K–T material from Blake Nose derives from the fallout of the material generated by the Chicxulub impact. Reworking of the impact-generated material downslope prevents a precise determination of the original thickness and limits evidence for inferring precise ejecta material distribution NE of Chicxulub. It does, however, provide evidence of the large volume of ejecta material reaching Blake Nose Plateau.

When compared with proximal ejecta, the spherules from Blake Nose are similar to spherules from different locations on the North America Atlantic margin, such as Bass River and Deep Sea Drilling Project (DSDP), 603B (Fig. 1). At Hole 603B, Klaver *et al.* (1987) reported green spherules in the lower part of a turbidite section that were also composed of smectite. The green spherules from Blake Nose (Site 1049) represent the same diagenetically altered impact ejecta from the Chicxulub crater. Spherules recovered at DSDP Hole 603B are spherical, with smooth or nodular morphologies, and they are massive or hollow (Klaver *et al.* 1987). At Bass River,

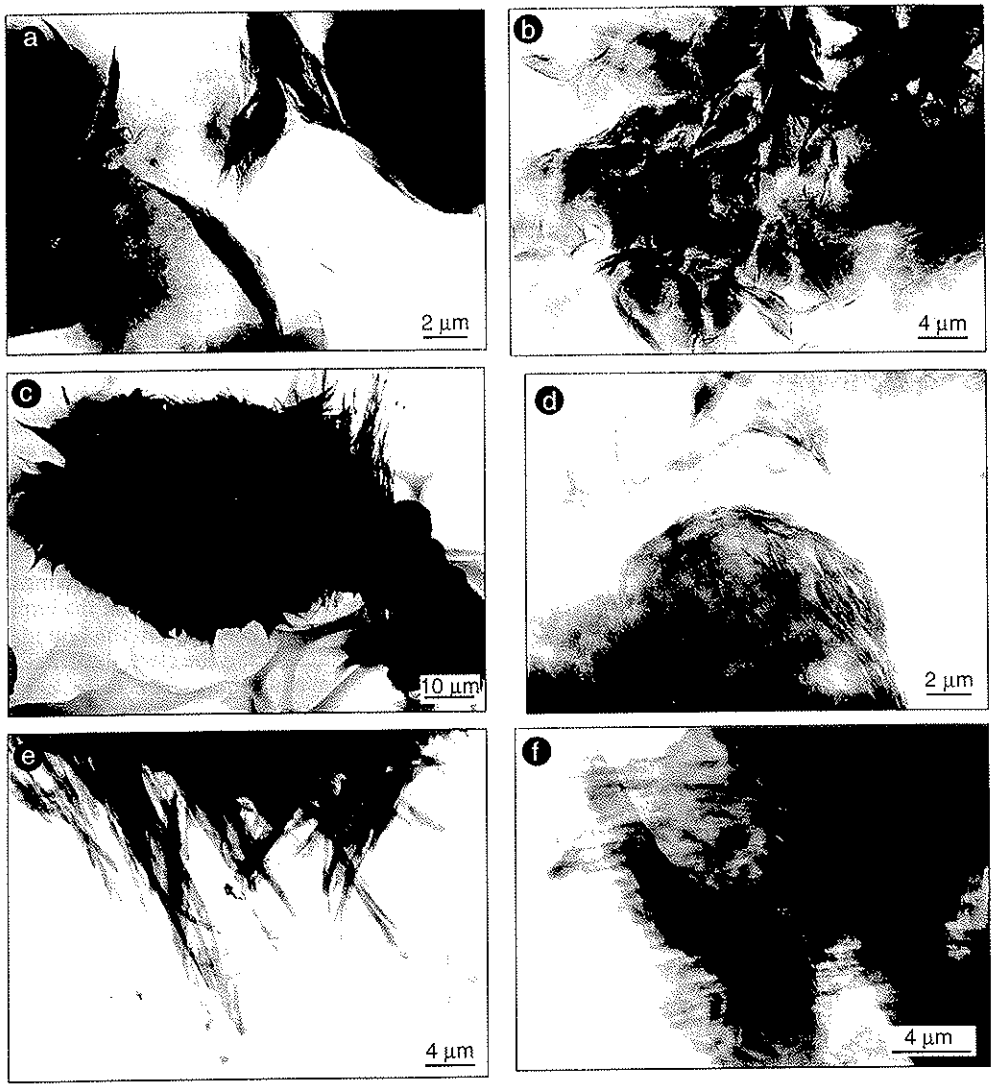

Fig. 7. Selected transmission electron micrographs of smectites from the spherule bed at Site 1049. (**a, b**) Hair-like smectite, which has replaced the original spherule glass. (**c**) Authigenic smectite replacing glass with some filmy veils and palygorskite fibres forming from smectite. (**d**) Smectites forming from a high-silica material, probably the altering glass. (**e, f**) Higher-resolution micrographs showing the authigenesis of palygorskite fibres.

New Jersey, the ODP Leg 174AX recovered a K–T interval with a 6 cm thick spherule bed (Miller *et al.* 1998). The spherule bed represents the altered impact ejecta and consists of a coarse and poorly graded unit containing spherical and oval-shaped spherules. These spherules have a smooth outer surface, a thin solid rim and a fine matrix containing in turn rounded spherules (Olsson *et al.* 1997). Spherules from the El Mimbral and La Lajilla sections (Smit *et al.* 1992; Keller *et al.* 1994) in Mexico are also similar but often contain a preserved impact glass core. Clay spheroids from Albion Island (Fig. 1) are also advocated to be impact glass (Ocampo *et al.* 1996; Pope *et al.* 1999). In Haiti, exposures of the ejecta deposits reveal spherules that are not completely altered, consisting of impact glasses and glass spherules (e.g. Izett 1991; Koeberl & Sigurdsson 1992).

The spherule bed recovered in the NW Atlantic at Bass River, DSDP Hole 603B and Blake Nose represent similar ejecta blanket deposits from the Chicxulub impact. The thickness of the spherule bed at Bass River is consistent with the southeast

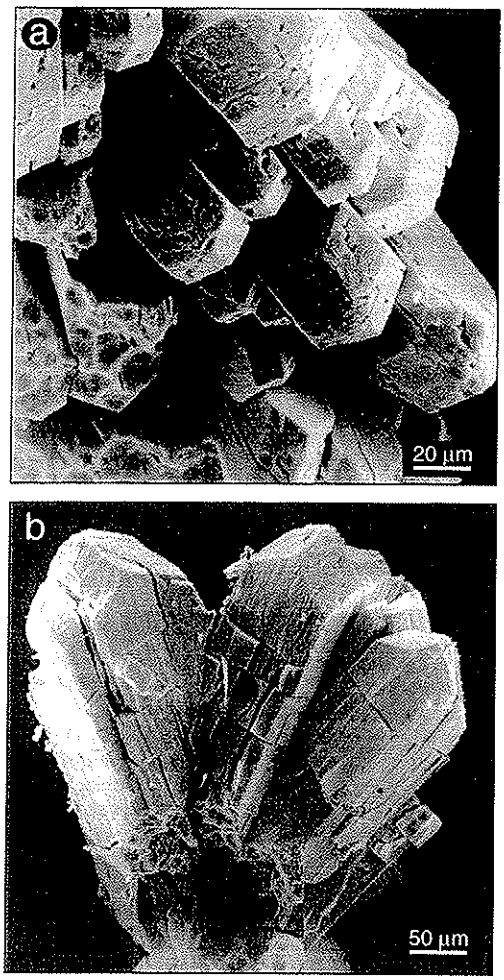

Fig. 8. Scanning electron micrographs of zeolites from the spherule bed at Site 1049.

low-angle impact hypothesis (Schultz & D'Hondt 1996) according to Olsson *et al.* (1997).

When comparing Blake Nose spherules and others from proximal sites (tektites and impact glasses) with those found at distal sites, it is found that their nature is very different. At distal sites spherules show evidence of a crystalline phase and quench-crystal textures, and, altered or not, are considered as microkrystites (Smit *et al.* 1992). At distal sections such as those at Agost and Caravaca (SE Spain), which are some of the most complete K–T boundary outcrops, the ejecta layer is mostly composed of smectite with abundant spherules, which are microkrystites according to the term proposed by Glass & Burns (1988). The ejecta deposits at these sections record a significant extraterrestrial contamination (Smit 1990; Martínez-Ruiz *et al.* 1997). Thus, the spherule bed at Blake Nose records mainly the terrestrial material involved in the impact. In contrast, distal ejecta deposits contain microkrystites and higher extraterrestrial contributions. The existence of tektites and microkrystites in the K–T boundary layer at proximal and distal sequences (Smit *et al.* 1992; Smit 1999) further supports the Chicxulub impact and patterns of global distribution of the impact-generated materials.

Conclusions

Spherules from the K–T ejecta deposits at Blake Nose derive from the impact material generated at the Chicxulub crater site. The original material has been altered to smectite. Mineralogical and geochemical evidence indicates that the smectites derive from the alteration of Si-rich and Ca-rich glass. During diagenetic processes, other mineral phases such as zeolites and palygorskite originated. Although the spherule bed resulted from reworking of the impact-generated material downslope, the ejecta deposit at ODP Site 1049 confirms that a large volume of this material that reached the Blake Nose Plateau.

We thank the ODP Leg 171B Shipboard Scientific Party and the crew of the *JOIDES Resolution* for assistance with the samples and data, and the Bremen ODP Core Repository for assistance during the sampling party. One of the authors (F. Martínez-Ruiz) thanks the University of Granada and 'Junta de Andalucía' for financial support for participation on ODP Leg 171B. This work was partially supported by Project PB96-1429 (DGES, MEC, Spain) and Research Group RNM0179 (Junta de Andalucía, Spain). We thank the C.I.C. (University of Granada, Spain) for the use of the analytical facilities. We also thank P. Sánchez-Gómez, I. Nieto and E. Abarca for their help in the laboratory. We also thank M. Dubois and P. Claeys for constructive reviews and the improvement of this paper.

References

ALVAREZ, W., CLAEYS, P. & KIEFFER, S. 1995. Emplacement of Cretaceous–Tertiary boundary shocked quartz from Chicxulub crater. *Science*, **269**, 930–935.

ALVAREZ, W., SMIT, J., LOWRIE, W. *et al.* 1992. Proximal impact deposits at the Cretaceous–Tertiary boundary in the Gulf of Mexico: a restudy of DSDP Leg 77 Sites 536 and 540. *Geology*, **20**, 697–700.

BECK, K. C. & WEAVER, C. E. 1978. Miocene of the S.E. United States: a model for chemical sedimentation in a peri-marine environment. Reply. *Sedimentary Geology*, **21**, 154–157.

BLUM, J. D., CHAMBERLAIN, C. P., HINGSTON, M. P. & KOEBERL, C. 1993. Isotopic composition of K–T boundary impact glass with melt rock from Chicxulub and Manson impact structures. *Nature*, **364**, 325–327.

BRALOWER, T. J., PAULL, C. K. & LECKIE, R. M. 1998. The Cretaceous–Tertiary boundary cocktail: Chicxulub impact triggers margin collapse and extensive sediment gravity flows. *Geology*, **26**, 331–334.

CHAMLEY, H. 1989. *Clay Sedimentology*. Springer, Berlin.

COUTURE, R. A. 1977. Composition and origin of palygorskite-rich and montmorillonite-rich zeolite-containing sediments from the Pacific Ocean. *Chemical Geology*, **21**, 149–153.

GLASS, B. P. & BURNS, C. A. 1988. Microkrystites: a new term for impact-produced glassy spherules containing primary crystallites. *In*: RYDER, S. (ed.) *Lunar and Planetary Science Conference, 18*, Pergamon, New York, 455–458.

GÜVEN, N. 1988. Smectites. *In*: BAILEY, S. W. (ed.) *Hydrous Phyllosilicates (Exclusive of Micas)*. Mineralogical Society of America, Reviews in Mineralogy, **19**, 497–559

HALL, A. 1998. Zeolitization of volcaniclastic sediments: the role of temperature and pH. *Journal of Sedimentary Research*, **68**, 739–745.

HILDEBRAND, A. R., PEWNFIELD, G. T., KRING, D. A., PILKINGTON, M., CAMARGO, Z. A., JACOBSEN, S. B. & BOYNTON, W. V. 1991. Chicxulub Crater: a possible Cretaceous–Tertiary boundary impact crater on the Yucatan Peninsula, Mexico. *Geology*, **19**, 867–871.

HOUGH, R. M., WRIGHT, I. P., SIGURDSSON, H., PILLINGER, C. T. & GILMOUR, I. 1998. Carbon content and isotopic composition of K–T impact glasses from Haiti. *Geochimica et Cosmochimica Acta*, **62**, 1285–1291.

IZETT, G. A. 1991. Tektites in Cretaceous/Tertiary boundary rocks on Haiti and their bearing on the Alvarez impact extinction hypothesis. *Journal of Geophysical Research*, **96**, 20879–20905.

JONES, B. F. & GALÁN, E. 1988. Sepiolite and palygorskite. *In*: Bailey, S. W. (ed.) *Hydrous Phyllosilicates (Exclusive of Micas)*. Mineralogical Society of America, Reviews in Mineralogy, **19**, 631–674.

KELLER, G., STINNESBECK, W. & LÓPEZ-OLIVA, J. G. 1994. Age, deposition, and biotic effects of the Cretaceous/Tertiary boundary event at Mimbral, NE Mexico. *Palaios*, **9**, 144–157.

KLAVER, G. T., VAN KEMPEN, T. M. G., BIANCHI, F. R. & VAN DER GAAST, S. J. 1987. Green spherules as indicators of the Cretaceous/Tertiary boundary in Deep Sea Drilling Project Hole 603B. *In*: VAN HINTE, J. E., WISE, S. W. Jr, *et al.* (eds) *Initial Reports of the Deep Sea Drilling Project*, **93**, US Government Printing Office, Washington, DC, 1039–1056.

KOEBERL, C. 1993. Chicxulub Crater, Yucatan: tektites, impact glasses, and the geochemistry of target rocks and breccias. *Geology*, **21**, 211–214.

KOEBERL, C. & SIGURDSSON, H. 1992. Geochemistry of impact glasses from the K–T boundary in Haiti: relation to smectites and a new type of glass. *Geochimica et Cosmochimica Acta*, **56**, 2113–2129.

MACDOUGALL, J. D. 1988. Seawater strontium isotopes, acid rain, and the Cretaceous–Tertiary boundary. *Science*, **239**, 485–487.

MARTIN, E. E. & MACDOUGALL, J. D. 1991. Seawater Sr isotopes at the Cretaceous–Tertiary boundary. *Earth and Planetary Science Letters*, **104**, 166–180.

MARTÍNEZ-RUIZ, F., ORTEGA-HUERTAS, M., KROON, D., SMIT, J., PALOMO-DELGADO, I. & ROCCHIA, R. 2001. Geochemistry of the Cretaceous–Tertiary boundary at Blake Nose (ODP Leg 171B). *This volume*.

MARTÍNEZ-RUIZ, F., ORTEGA-HUERTAS, M., KROON, D. & ACQUAFREDDA, P. 1997. Quench textures in altered spherules from the Cretaceous–Tertiary boundary layer at Agost and Caravaca, SE Spain. *Sedimentary Geology*, **113**, 137–147.

MILLER, K. G., SUGARMAN, P. J., BROWNING, J. V. *et al.* (eds) 1998. *Proceedings of the Ocean Drilling Program, Initial Reports*, **174AX**. Ocean Drilling Program, College Station, TX.

NIETO, F., LÓPEZ-GALINDO, A. & PEINADO-FENOLL, E. 1989. *Programa de recogida de datos del difractómetro de rayos X*. Departamento de Mineralogía y Petrología, Universidad de Granada.

NIETO, F., ORTEGA-HUERTAS, M., PEACOR, D. R. & AROSTEGUI, J. 1996. Evolution of illite/smectite from early diagenesis through incipient metamorphism in sediments of the Basque–Cantabrian basin. *Clays and Clay Minerals*, **44**, 304–323.

NORRIS, R. D., HUBER, B. T. & SELF-TRAIL, J. 1999. Synchroneity of the K–T oceanic mass extinction and meteorite impact: Blake Nose, Western North Atlantic. *Geology*, **27**, 419–422.

NORRIS, R. D., KROON, D., KLAUS, A. *et al.* 1998. *Proceedings of the Ocean Drilling Program, Initial Reportsn*, **171B**. Ocean Drilling Program, College Station, TX, 47–91.

OCAMPO, A. C., POPE, K. O. & FISCHER, A. G. 1996. Ejecta blanket deposits of the Chicxulub crater from Albion Island, Belize. *In*: RYDER, G., FASTOVSKY, D. & GARTNER, S. (eds) *The Cretaceous–Tertiary Event and Other Catastrophes in Earth History*. Geological Society of America, Special Papers, **307**, 75–88.

OLSSON, R. K., MILLER, K. G., BROWNING, J. V., HABIB, D. & SUGARMAN, P. J. 1997. Ejecta layer at the Cretaceous–Tertiary boundary, Bass River, New Jersey (Ocean Drilling Program Leg 174AX). *Geology*, **25**, 759–762.

PIERAZZO, E. & MELOSH, J. H. 1999. Hydrocode modeling of Chicxulub as an oblique impact event. *Earth and Planetary Science Letters*, **165**, 163–176.

POPE, K. O., OCAMPO, A. C., FISCHER, A. G. *et al.* 1999. Chicxulub impact ejecta from Albion Island, Belize. *Earth and Planetary Science Letters*, **170**, 351–364.

RETALLACK, G. J. 1996. Acid trauma at the Cretaceous–Tertiary boundary in Eastern Montana. *GSA Today*, **6**, 1–7.

SCHULTZ, P. H. & D'HONDT, S. 1996. Cretaceous–Tertiary (Chicxulub) impact angle and its consequences. *Geology*, **24**, 963–967.

SHARPTON, V. L., BURKE, K., CAMARGO-ZANOGUERA, A. *et al.* 1993. Chicxulub multiring impact basin: size and other characteristics derived from gravity analyses. *Science*, **261**, 1564–1567.

SIGURDSSON, H., D'HONT, S., ARTHUR, M. A., BRALOWER, T. J., ZACHOS, J. C., VAN FOSSEN, M. & CHANNELL, E. T. 1991. Glass from the Cretaceous/Tertiary boundary in Haiti. *Nature*, **349**, 482–487.

SIGURDSSON, H., D'HONT, S. & CAREY, S. 1992. The impact of the Cretaceous/Tertiary bolide on evaporite terrane and generation of major sulfuric acid aerosol. *Earth and Planetary Science Letters*, **109**, 543–559.

SINGER, A. 1979. Palygorskite in sediments: detrital, diagenetic or neoformed. A critical review. *Geologsche Rundschau*, **68**, 996–1008.

SMIT, J. 1990. Meteorite impact, extinctions and the Cretaceous–Tertiary boundary. *Geologie en Mijnbouw*, **69**, 187–204.

SMIT, J. 1999. The global stratigraphy of the Cretaceous–Tertiary boundary impact ejecta. *Annual Review of Earth and Planetary Sciences*, **27**, 75–113.

SMIT, J., MONTANARI, A., SWINBURNE, N. H. S. *et al.* 1992. Tektite-bearing, deep-water clastic unit at the Cretaceous–Tertiary boundary in northeastern Mexico. *Geology*, **20**, 99–103.

SWISHER, C. C., GRAJALES, N. J. M., MONTANARI, A. *et al.* 1992. Coeval $^{40}Ar/^{39}Ar$ ages of 65.0 million years from Chicxulub melt rock and Cretaceous–Tertiary boundary tektites. *Science*, **257**, 954–958.

VELDE, B. 1985. *Clay Minerals. A Physical-Chemical Explanation of their Occurrence.* Elsevier, Amsterdam.